MARTIAN REGOLITH PROPERTIES: VIKING IRTM SPECTRAL DIFFERENCING RESULTS. P.R. Christensen, Dept. of Earth & Space Science, Univ. of Calif., Los Angeles, CA 90024.

During the lifetime of the Viking orbiters, Infrared Thermal Mapping (IRTM) observations were made of Mars in four surface-sensing thermal bands centered at 7, 9, 11 and 20 μm and in a 0.3 to 3.0 μm solar reflectance band. Much of the surface property analysis to date has been directed toward the determination of the thermal inertia (I), ($I = (k\rho c)^{\frac{1}{2}}$, where k is the thermal conductivity, ρ is the density and c is the specific heat) using the observed 20 μm temperature (T_{20}) and the measured Lambert albedo (1,2). While this determination represents a significant advancement in the understanding of the surface character, it does not provide a unique solution to the size distribution of the surface materials, since the thermal inertia is a measure of the average grain size, not the distribution of grain sizes present. We have investigated this ambiguity by studying the differences in brightness temperature between the IRTM thermal bands. These spectral differences are due to departures of the surface from an ideal blockbody, either through the mixture within the field of view of surface materials of different sizes and therefore at different kinetic temperatures or through a variation in the emissivity of the surface material with wavelength.

Using numerical thermal models (3) to predict the diurnal variation of temperature for materials of different thermal inertia, albedo and emissivity, these temperatures are converted to flux, combined in varying proportions and reconverted to brightness temperatures in each IRTM band. In addition, the resultant 20 μm temperature is used in a manner identical to that used by Palluconi and Kieffer (2) to determine the effective thermal inertia. By comparing the observed diurnal variation of the temperature differences between bands with this model and by constraining the effective inertia to agree with that obtained by Palluconi and Kieffer (2) for the same area, the block population, thermal inertia of the fine component and thermal emissivity of the regolith can be estimated. An example of this modeling is shown in Figures 1a and b along with data from the Arabia low inertia region (latitude 26 - 36°, longitude 318 - 338°) collected into 1/4 hour bins. The models are quite sensitive to variations in these parameters. In addition, the diurnal signatures of anisothermality and emissivity are markedly different, allowing a separation of the two effects. Differences due to anisothermality are greatest at night because of the increased non-linearity of the Planck function at lower temperatures at the IRTM wavelengths and go to zero at dawn and dusk when materials of different thermal inertia have nearly the same kinetic temperature and the surface anisothermality is negligible. In contrast, as the spectral differences due to emissivity are proportional to temperature, they reach a maximum near noon and are always non-zero.

At present the complicating effects of a dusty atmosphere have not been explicitly included. These effects have been studied (4,5) for variations of optical depth, thermal inertia, and albedo. Preliminary work indicates that dust is not a dominant effect, as the diurnal spectral signature produced by a dusty atmosphere peaks near noon, in contrast with the observed variation. In addition, the data shown here were acquired during the northern summer season, when the infrared optical depth was approximately 0.1 (6).

In the Arabia region, the best fit of this model to the data is obtained for a regolith composed of an inertia 2.0 (units of 10^{-3} cal cm^{-2} $sec^{-\frac{1}{2}}$ K^{-1} assumed) fine component and with 2 - 3% areal coverage of inertia 30 (~10 cm) rocks, giving an effective thermal inertia of 2.4. Thermal emissivities at 7, 11 and 20 μm are nearly unity. The presence of rocks is significant because it implies that even the low inertia regions are not completely mantled by fine material. The maximum areal rock cover found in the northern equatorial region using this technique is approximately 10%. Therefore, the low inertia regions do not have substantially lower rock abundances than other areas. Instead, the difference appears to be a variation in the inertia of the regolith fine component which may be due to real variations in grain size or to variations in the degree of bonding.

Analysis of the IRTM data has also discovered a strong linear correlation of spectral differences with albedo for noontime data (Fig. 2). As spectral differences at this time of day are most sensitive to emissivity variations, this observation suggests a strong correlation of emissivity with albedo. The linearity of the variation suggests a surface composed of a mixture of a small number of components whose relative fractions vary continuously. For example, as low emissivity produces daytime spectral differences, the surface may be composed of mixtures of a dark, low emissivity component and a bright, high emissivity component. This could be due either to a mineralogic difference between the bright and dark materials, or to the mutual dependence of emissivity and albedo on grain size. In this latter case, both the albedo and the emissivity are known to decrease with increasing grain size (7,8), producing a relationship similar to that seen in Figure 2.

SUMMARY

It appears that spectral differencing will allow an estimation of the block fractions present on the surface of Mars. In the areas studied, no region has been found with more than 5 - 10% nor less than 2% areal rock cover. This implies that the major difference between high and low inertia areas is not the abundance of blocks but rather the inertia of the fine component of the regolith. This places some doubt on preferential dust deposition within the low inertia regions as the sole explanation for these features. In addition, there is a strong correlation of Lambert albedo with thermal emissivity. This may be due to mineralogic differences between high and low albedo materials or to the dependence of both albedo and emissivity on grain size.

REFERENCES

(1) Christensen, P.R. and H.H. Kieffer (1979) J. Geophys. Res., 84, p. 8233-8238.

(2) Palluconi, F.D. and H.H. Kieffer (1981) Icarus, in press.

(3) Kieffer, H.H. et al. (1977) J. Geophys. Res., 82, p. 4249-4291.

(4) Jakosky, B.M. (1979) J. Geophys. Res., 84, p. 8252-8262.

(5) Davies, D.W. (1979) J. Geophys. Res., 84, p. 8289-8293.

(6) Pleskot, L.K. and E.D. Miner (1981) Icarus, in press.

(7) Hapke, B. (1963) J. Geophys. Res., 68, p. 4571.

(8) Hovis, W.A., Jr. and W.R. Callahan (1966) J. Opt. Soc. Am., 56, p. 639-643

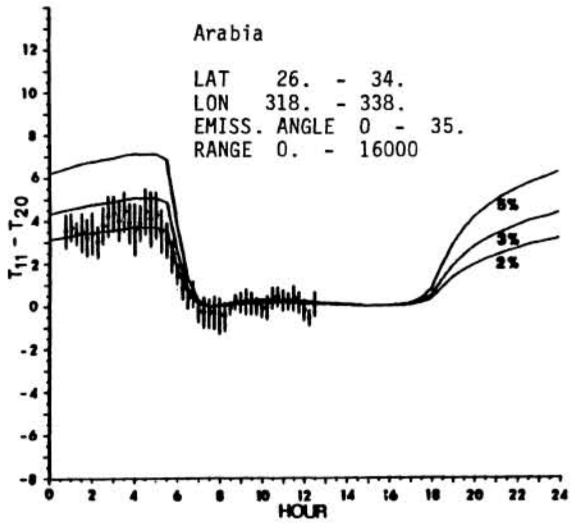

FIGURE 1a - The spectral variation of $T_{11} - T_{20}$ as a function of time juxtaposed with models of the spectral variation due to block fraction. For the Arabia region it suggests that 2 - 3% of the surface is covered by rocks greater than 30 cm. Vertical bars are the 2 sigma variation within each bin. Model curves assume a regolith composed of a fine component having a thermal inertia of 2.0, an albedo of 0.25 and unit thermal emissivity, and blocks having an inertia of 30.0, albedo of 0.10 and unit emissivity.

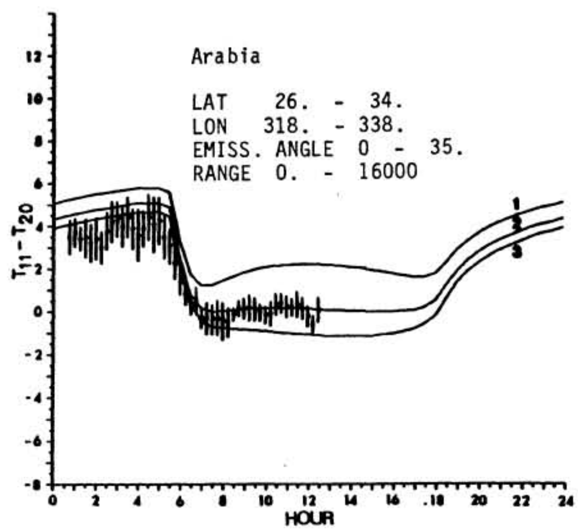

FIGURE 1b - The same data juxtaposed with models of the spectral variation due to non-unit emissivities of the fine component. Thermal inertia and albedo values are the same as Figure 1a. In curve 1, the 11 µm emissivity (ε_{11}) is 1.0, 20 µm emissivity (ε_{20}) is 0.98. In curve 2, $\varepsilon_{11} = 1.0$, $\varepsilon_{20} = 1.0$. In curve 3, $\varepsilon_{11} = 0.98$, $\varepsilon_{20} = 1.0$. In all cuves the block cover is 2%. For the Arabia region ε_{11} and ε_{20} are approximately unity.

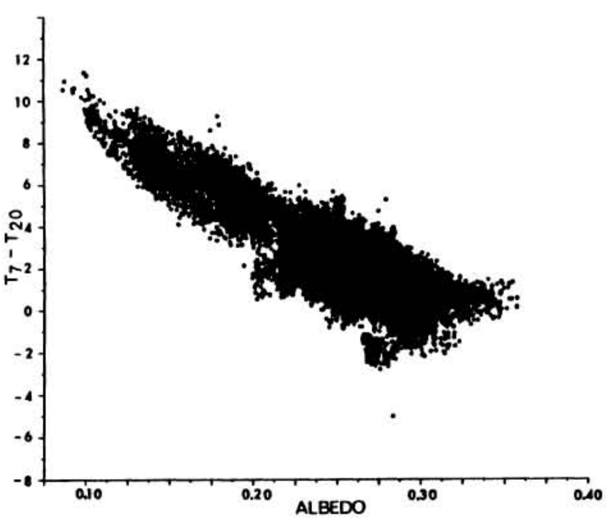

FIGURE 2 - The spectral variation of $T_7 - T_{11}$ as a function of Lambert albedo for noontime data. Spectral differences, which are due to emissivity at this time of day, show a strong correlation with albedo. Data are from Viking 1 orbits 579 to 640 (L_s 34.8° to 61.9°) covering the northern hemisphere (0 - 30°N latitude, 0 - 360°W longitude). All data were constrained with local time between 11.5 H and 12.5 H, emission angle less than 35° and range less than 16,000 km.